Int. J. Heat Mass Transfer. Vol. 34, No. 4/5, pp. 1105–1111, 1991
Printed in Great Britain

0017-9310/91 $3.00+0.00

Evaporative cooling of liquid film through interfacial heat and mass transfer in a vertical channel—I. Experimental study

W. M. YAN, T. F. LIN and Y. L. TSAY
Department of Mechanical Engineering, National Chiao Tung University, Hsinchu, Taiwan 30050, R.O.C.

(*Received* 16 *August* 1989 *and in final form* 5 *June* 1990)

Abstract—An experimental study is performed to study the evaporative cooling of the falling liquid film through interfacial heat and mass transfer in a vertical channel. The measured wall temperature, heat and mass transfer rates are specifically presented for the systems with water film evaporation and ethanol film evaporation over wide ranges of liquid mass flow rate, channel width and liquid inlet temperature. The results show that the influences of the evaporative latent heat transfer on the cooling of the liquid film depend largely on the inlet liquid film temperature and liquid mass rate. Effective evaporative cooling results for a higher inlet liquid film temperature and a smaller liquid mass flow rate.

1. INTRODUCTION

MOMENTUM, solutal and thermal interactions between falling liquid films along vertical channel surfaces and gas/vapour streams are widely encountered in industrial applications. Windy-day evaporation and vaporization of mist and fog, distillation of a volatile component from a mixture with involatiles, the process of evaporative cooling for waste heat disposal, and cooling of a high temperature surface by coating it with phase-change material are just some prominent examples of such processes in which mass transfer operations are accompanied by the transfer of heat.

Heat transfer in buoyancy-driven channels flows has been studied in detail [1–4]. The effects of mass diffusion on natural convection heat transfer have been widely examined for external flows [5–8] and internal flows [9–11]. As far as mixed convection is concerned, the influence of the wetted wall on laminar mixed convection heat transfer in a vertical channel was investigated in refs. [12–14]. In refs. [10–14], it was found that heat transfer on the gas side is dominated by the transport of latent heat in association with the evaporation of the liquid film. For forced convection heat and mass transfer, studies have been carried out for flows over a flat surface [15, 16] and a wedge [17] and for flows in a channel [18].

The studies [10–18] just reviewed above all focus on the heat and mass transfer in the gas/vapour stream but all neglect the liquid film thickness on the wall. The results thus produced are only good for the system with an extremely thin film. In practical situations, the liquid film on the wall is finite in thickness, and thereby the influences of the momentum and energy transport in the liquid film on the heat and mass transfer in the gas flow should be considered in the analysis. Recently, Suzuki *et al.* [19], Baumann and Thiele [20] and Shembharkar and Pai [21] examined the effects of finite film thickness on the heat and mass transfer in forced convection flows. In their studies [19–21], the Nusselt type approximation was made to simplify the analysis of the liquid film. The results show that the liquid film can be used as a heat barrier to the hot gas stream [21]. Recently, the evaporation rates of water were measured by Haji and Chow [22] and the measured data agree well with the predicted results [15] if the heat loss from the water pan is accounted for. In addition, a steady, one-dimensional model of heat and mass transfer in a single-tube evaporative cooler was formulated in ref. [23] and validated experimentally. Conder *et al.* [24] studied the vaporization of a liquid film flowing orderly down the inside surface of a smooth tube into a countercurrent, laminar flow of gases.

Despite the fact that the combined heat and mass transfer in natural convection between vertical parallel plates with film evaporation is relatively important in engineering applications, it has not received much attention. The main objective of the present study is to perform an experimental study to examine the evaporative cooling of a falling liquid film through interfacial heat and mass transfer in a vertical channel.

2. EXPERIMENTAL STUDY

The experimental set-up for investigating the evaporative cooling in a vertical channel is schematically shown in Fig. 1. The channel walls are made of stainless steel SS304 plate sheets 1 m long, 30 cm wide, and 1 mm thick. In order to support the test section and prevent the heat loss from the test section to the ambient, low thermal conductivity balsa wood plates 1.5 cm thick are glued on the outside surfaces of the steel plates. As indicated in Fig. 1, the liquid to be cooled falls down along the inside surfaces of the channel

NOMENCLATURE

B	liquid mass flow rate per unit periphery length at inlet	T_w	wall temperature
b	half channel width	x	coordinate in the flow direction.
c_p	specific heat	Greek symbols	
h_{fg}	latent heat of evaporization	λ	molecular thermal conductivity
l	channel length	ρ	density.
q''_I	average interfacial heat flux on gas side		
t	thickness of the balsa wood	Subscripts	
T	temperature	I	condition at the gas–liquid interface
T_{li}	inlet liquid film temperature	l	liquid film
T_{lo}	outlet liquid film temperature	o	ambient condition or inlet condition.

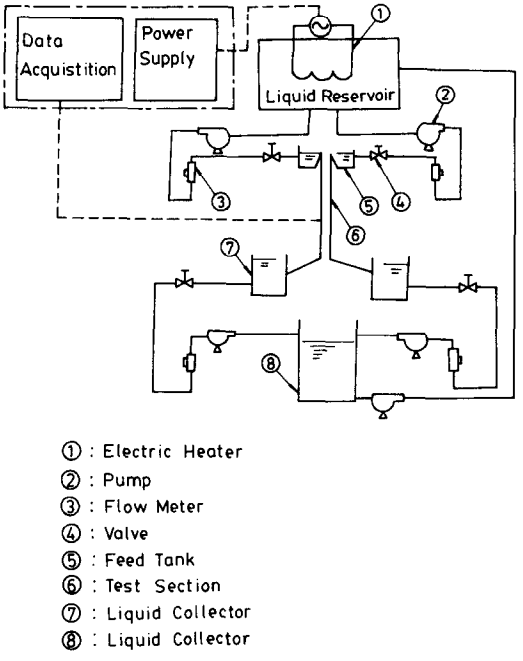

FIG. 1. System of falling film fluid delivery.

walls from the feed tanks. The liquid leaving the outlet of the channel (bottom end) is collected and pumped to the liquid reservoir. In the liquid reservoir the liquid is indirectly heated by a heating system. To accurately control the temperature of the liquid in the tank, an automatic feedback heating system which comprises a very sensitive Pt rod, a temperature controller and a power regulator is used.

2.1. *Measurement of channel wall temperature*

Direct measurement of the velocity and temperature distributions in the liquid film and gas stream and the liquid film thickness will provide the detailed heat and mass transfer characteristics during the evaporative cooling process. This is, however, still a very difficult task at the present time. Instead, a simple experiment is performed to illustrate the integral heat and mass transfer characteristics. Measurement of the plate temperature gives the liquid film temperature distribution since the temperature variation across the thin liquid film considered here is relatively small [25]. In addition, the total evaporation rate of the liquid film is obtained by an indirect method to be described in Section 2.2.

The wall temperature along the test section is measured with the copper–constantan thermocouples (T-type). The arrangements of the thermocouples on the left channel wall are spaced 50 or 100 mm apart longitudinally. The first thermocouple is fixed 55 mm away from the top end while the last thermocouple is attached at the bottom end of the test section. At three axial locations along the vertical plate, three thermocouples are fixed across the spanwise section of the channel to check the circumferential uniformity of the wall temperature, that is, to indirectly check the spanwise uniformity of the liquid film thickness across the test section at every streamwise location. As for the right channel wall, the thermocouples are spaced 100 mm apart in the streamwise direction. Prior to the installation the thermocouples are calibrated by the LAUDA compact low-temperature thermostats (type RKS 20-D) with a YEW digital thermometer (type 2575). The overall accuracy of the thermocouples is believed to be well within 0.2°C.

Due to the heat loss from the insulation, the measured wall temperature needs to be corrected. This is done by measuring the outer surface temperature of the insulation and by using the following equation to correct the measured wall temperature:

$$T_w = T'_w + \frac{1}{Bc_p}\int_0^x q''_{loss}\,dx \qquad (1)$$

where T'_w is the measured wall temperature, B the inlet liquid mass flow rate and q''_{loss} the heat loss from the insulation. Notice that equation (1) is obtained by applying the energy balance to a control volume of the test section including the wall and the liquid film and by employing the lumped system analysis.

To facilitate the analysis, the heat loss is estimated by assuming linear temperature variation through the insulation

$$q''_{\text{loss}} = \lambda_{\text{ins}} \frac{T_w - T_{wo}}{t} \quad (2)$$

where T_{wo} is the outer surface temperature of the insulation, t the thickness of the insulation and λ_{ins} the thermal conductivity of balsa wood which is evaluated from the equation [26]

$$\lambda_{\text{ins}} = -1.164 \times 10^{-6} \rho^2 + 7.108 \times 10^{-4} \rho - 0.02514 \ (\text{W m}^{-1}\text{K}^{-1}) \quad (3)$$

where ρ(kg m^{-3}) is the density of the balsa wood.

Because binary diffusion and heat transfer in a vertical channel with symmetric conditions are examined in the present study, the spanwise uniformity of the liquid film along the channel and the symmetries in the liquid film temperature and liquid mass flow rate at the right and left channel walls are important. To assess the uniformity of the liquid film along the channel, three thermocouples are installed at three longitudinal locations spanwisely across the test section. To sustain the uniformity, the test sections are treated by rubbing the plate surfaces with emery paper in each experimental run to ensure the measured wall temperature differences among these locations at the same x being less than 0.2°C. Therefore, we have the confidence that the uniformity of the liquid film across the test section can be obtained.

To get the symmetric conditions at the two channel walls, the symmetric system set-up with symmetric pipe lines is designed (see Fig. 1). In the experimental run, the maximum difference in the wall temperature at the same corresponding locations along the right and left walls is always less than 0.3°C.

2.2. *Measurement of liquid flow rate*

The liquid flow rates at the inlet and exit of the channel are measured by using Hsin Chuan variable area type flow indicators (M-type). These flowmeters are calibrated by measuring the flow output of the system over a specified interval of time at different float positions. Such measurement is carried out at several liquid temperatures so that the effect of property variations with temperature is taken into account. Flowmeter calibration curves are thereby determined for all flowmeters and fluids tested here—water and ethanol. With the liquid flow rates measured at the inlet and outlet, the total mass evaporation rate from the liquid film to the gas stream can be obtained. But during the experimental run, it was found that the amount of the mass evaporation is very small and is less than 4% of the inlet liquid mass flow rate B. This low value of mass evaporation rate is difficult to obtain accurately from the measured inlet and outlet liquid flow rates. Therefore, the results of the average mass evaporation rate are not presented here.

3. RESULTS AND DISCUSSION

In the present study, two different fluids are considered for the liquid film—water and ethanol. Water is chosen as the test fluid because it is often encountered in many applications, while high volatility is considered when choosing ethanol. The ranges of experimental conditions are listed in Table 1. Note that in Table 1, the relative humidity at the ambient ϕ and ambient temperature T_o are difficult to control at specified values during the experimental run. Therefore, the ranges of ϕ and T_o, listed in Table 1, are the ranges of all the experimental runs. The effect of ϕ on the heat and mass transfer during the evaporative process is insignificant except when ϕ is very small [10]. To clearly present the results, this section is divided into two parts. One gives the water film evaporation, while the other gives the ethanol film evaporation. In the present study only the experimental results are reported here, since the detailed numerical analysis for the problem is available in refs. [25, 27].

Table 1. The ranges of the physical parameters

	Water	Ethanol
Inlet liquid temperature, T_{li}(°C)	40 ~ 60	27 ~ 40
Inlet liquid mass flow rate, B(kg m^{-1} s^{-1})	0.03 ~ 0.06	0.01 ~ 0.04
Relative humidity of ambient air, ϕ(%)	70 ~ 90	80 ~ 90
Ambient temperature, T_o(°C)	30 ~ 31	T_o = 31.5°C as T_{li} = 40°C T_o = 30°C as T_{li} = 30°C T_o = 30.5°C as T_{li} = 27°C
Channel width, $2b$(m)	0.015 ~ 0.05	0.03
Channel length, l(m)	1.0	1.0

3.1. *Water film evaporation*

The measured, axial developments of water film temperature at the insulated wall are presented in Fig. 2 for a channel width $2b = 0.03$ m at different inlet liquid mass flow rates and inlet liquid film temperatures. An overall inspection of Figs. 2(a) and (b) reveals that the film temperature at the channel wall decreases monotonically along the channel. This feature can be made plausible by noting the fact that as the liquid film falls down along the channel surface, the high temperature water film evaporates. Meanwhile, there is sensible heat transfer from the liquid to the gas flow because $T_w > T_o$. Therefore, the energy required to sustain the evaporative latent heat transfer at the interface and sensible heat transfer to the gas flow must come from the internal energy of the liquid, resulting in a reduction in the liquid film temperature. Also clearly seen in Fig. 2 is that the larger the liquid mass flow rate, the smaller the temperature drop. This is simply due to the larger total internal energy possessed by the liquid film for a larger liquid mass flow rate (i.e. larger $Bc_p\Delta T_l$), which, in turn, results in a smaller temperature drop along the channel.

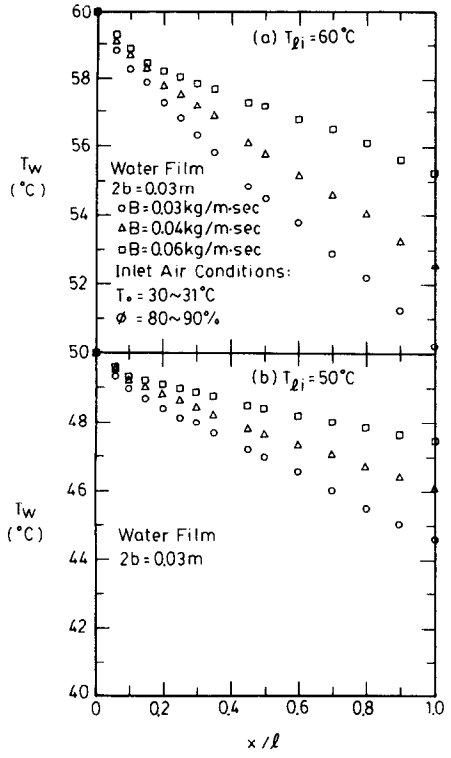

FIG. 2. Axial distributions of wall temperature for water film evaporation.

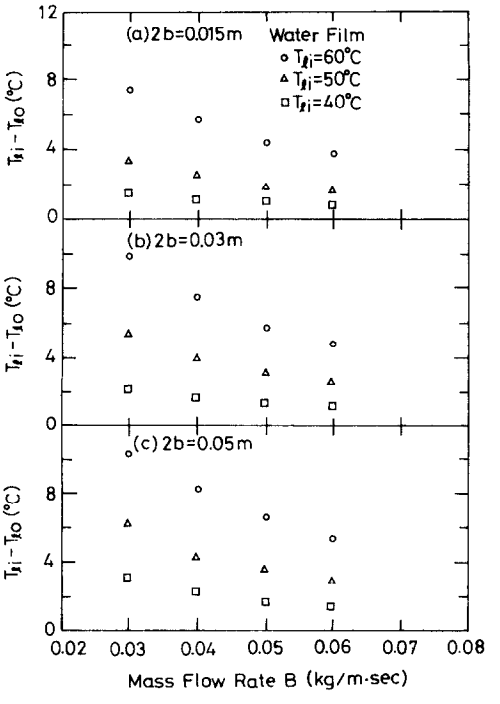

FIG. 3. Effect of inlet liquid temperature and mass flow rate on the temperature drops.

Comparing the corresponding curves in Figs. 2(a) and (b) indicates that larger temperature reduction is experienced for the system with a higher T_{li}. This results from the larger latent heat exchange associated with film vaporization together with the larger sensible heat exchange for the case with a higher T_{li}. In separate experimental runs, it was also found that the larger the interplate separation (channel width), the larger the liquid temperature drop. This confirms the fact that in natural convection heat transfer the energy transfer is more effective for the case with larger Grashof numbers connected with the larger channel width. Note that the Grashof numbers for heat and mass transfer are proportional to b^3 [10, 11].

In the study of evaporative cooling, the total temperature depression of the liquid film from the inlet to the outlet is one of the most important quantities. Figure 3 shows the measured total temperature drops in the liquid film at different conditions. As mentioned earlier, larger liquid temperature drops are experienced for the systems with larger T_{li} and b or smaller B. It is surprising to note that in Figs. 3(b) and (c) the temperature reduction for the case with $T_{li} = 60$°C and $B = 0.03$ kg m^{-1} s^{-1} can be as much as 10°C. This result suggests that the ideas of evaporative cooling due to the latent heat exchange in connection with film evaporation can be applied to the waste heat disposal in nuclear power plants and many other industries.

With the effects of T_{li}, b and B on the temperature drop of the liquid film examined, attention is now turned to the effects of these physical parameters on the average interfacial heat flux on the gas side. Figure 4 shows the results of the interfacial heat flux $\bar{q}_l''$ against inlet liquid mass flow rate B. In this plot the average interfacial heat flux is estimated by the following equation:

$$\bar{q}_l'' = Bc_p(T_{li} - T_{lo})/l. \tag{4}$$

The results show that larger $\bar{q}_l''$ is experienced for the case with a larger T_{li}. This is again due to the larger latent heat transfer for a higher T_{li}. Besides, these results also show that the magnitude of $\bar{q}_l''$ is as high as 10^3 W m^{-2}. This value is approximately ten times the average heat transfer rate without film evaporation under $T_w = T_{li}$. This says that, in the gas flow, the latent heat transport connected with film evaporation predominates over the sensible heat exchange.

It is more useful in applications if the experimental data for different conditions can be collapsed into a single curve. Figure 5 shows the curve-fitting results of the average interfacial heat flux. The relation is

$$\bar{q}_l'' = 0.0113\, T_{li}^{3.15} \cdot b^{1.3}. \tag{5}$$

It is noted that the correlation for $\bar{q}_l''$ is independent of the liquid mass flow rate B. This is readily understood if we check the results in Fig. 4, which show that the effect of B on $\bar{q}_l''$ is insignificant.

3.2. *Ethanol film evaporation*

Figure 6 shows the measured axial distributions of the liquid ethanol film temperature at the insulated

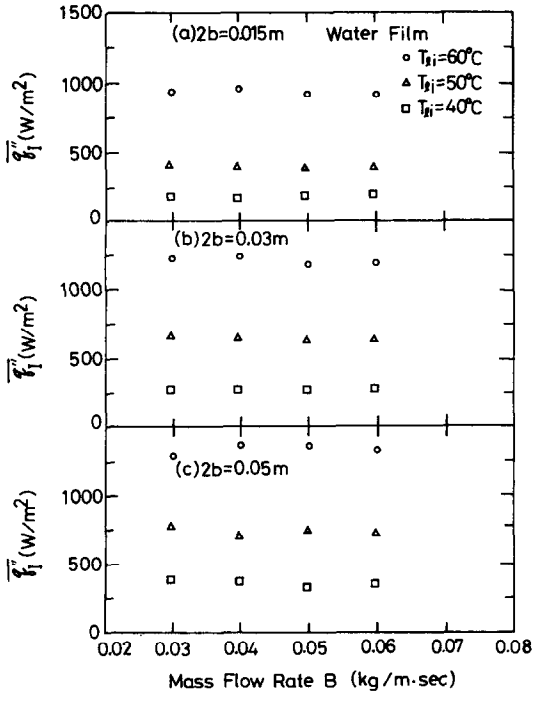

FIG. 4. Effects of inlet liquid temperature and mass flow rate on the average interfacial heat transfer rate.

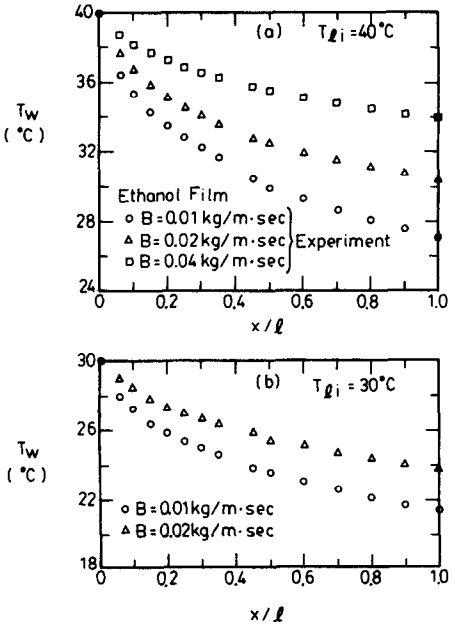

FIG. 6. Axial distributions of wall temperature along the channel.

wall. The upper plot corresponds to the results for $T_{li} = 40°C$ and $T_o = 31.5°C$ at different B while the lower plot is for $T_{li} = T_o = 30°C$ at different B. As the results shown in Fig. 2 for the water film evaporation, the insulated wall temperature decreases monotonically along the channel. The larger temperature depression along the channel is experienced for the case with a smaller B or higher T_{li}. It is worth noting that the outlet wall temperature for the case with $T_{li} = 40°C$ and $B = 0.01$ kg m^{-1} s^{-1} is below the ambient temperature. The total temperature drop of the liquid film is presented in Fig. 7 for different conditions. Like the results for the water film evaporation in Fig. 3, the higher the T_{li}, the larger the total temperature drop. This is due to more effective evaporative cooling for the case with a higher T_{li}. In addition, the larger temperature depression is also found for the case with a smaller liquid mass flow rate.

Figure 8 displays the results of the average interfacial heat flux for different conditions. It is clearly found in Fig. 8 that larger $\bar{q}_l''$ results for the case with a larger B. This results from the larger interfacial liquid film temperature for the case with larger B, which in turn causes a larger evaporative latent heat transfer. Moreover, larger $\bar{q}_l''$ also results for the system with a higher T_{li}. Comparing Fig. 8 with Fig. 4 indicates that the interfacial heat flux for the ethanol film is only slightly larger than that for the water film. This is simply due to the smaller latent heat of vaporization for ethanol.

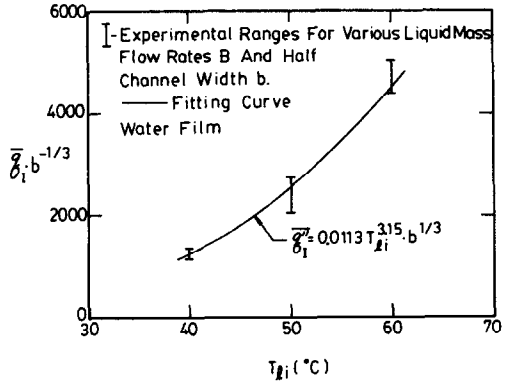

FIG. 5. Correlation of $\bar{q}_{sl}'' \cdot b^{-1/3}$ against T_{li} for water film evaporation.

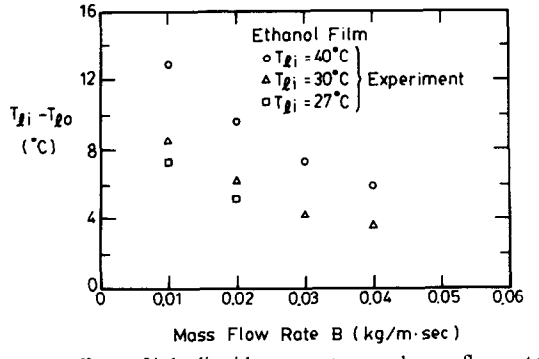

FIG. 7. Effects of inlet liquid temperature and mass flow rate on the temperature drops for ethanol film evaporation.

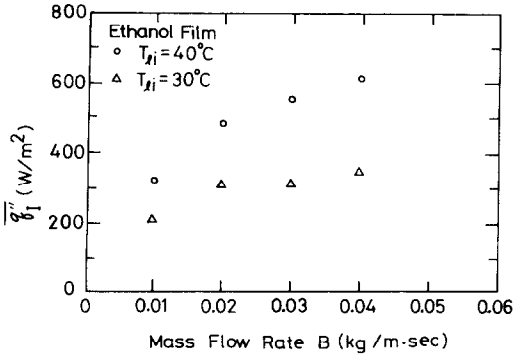

FIG. 8. Effects of inlet temperature and mass flow rate on the average interfacial heat transfer rate for ethanol film evaporation.

4. CONCLUSIONS

The evaporative cooling of the liquid film through interfacial heat and mass transfer has been experimentally studied. The effects of the system temperature, channel width and inlet liquid mass flow rate on the heat and mass transfer characteristics are examined in great detail. A brief summary of the major results is given below:

(1) Heat transfer in the gas side is dominated by the transport of latent heat in association with the evaporation of the liquid film.

(2) The influences of the evaporative latent heat transfer on the cooling of the liquid film depend largely on the inlet liquid film temperature T_{li} and inlet liquid mass flow rate B. Results show that the higher the T_{li} and the smaller the B, the larger the liquid film cooling.

(3) In the ranges of the experimental conditions, the average interfacial heat transfer rate for water film evaporation can be correlated by one equation

$$\overline{q_l''} = 0.0113\, T_{li}^{3.15} \cdot b^{1/3}. \quad (5)$$

Acknowledgement—The financial support of this research by the engineering division of National Science Council of Taiwan, R.O.C., through contract NSC77-0401-E009-10, is greatly appreciated.

REFERENCES

1. J. R. Bodoia and J. F. Osterle, The development of free convection between heated vertical plates, *J. Heat Transfer* **84,** 40–44 (1962).
2. W. Aung, L. S. Fletcher and V. Sernas, Developing laminar free convection between vertical flat plates with asymmetric heating, *Int. J. Heat Mass Transfer* **15,** 2293–2308 (1973).
3. A. Wirtz and R. J. Stutzman, Experiments on free convection between vertical plates with symmetric heating, *J. Heat Transfer* **104,** 501–507 (1982).
4. E. M. Sparrow and L. F. A. Azevedo, Vertical-channel natural convection spanning between the fully-developed limit and the single-plate boundary-layer limit, *Int. J. Heat Mass Transfer* **28,** 1847–1857 (1985).
5. W. M. Gill, E. D. Casal and D. W. Zeh, Binary diffusion and heat transfer in laminar free convection boundary layers on a vertical plate, *Int. J. Heat Mass Transfer* **8,** 1135–1151 (1965).
6. T. S. Chen and C. F. Yuh, Combined heat and mass transfer in natural convection along a vertical cylinder, *Int. J. Heat Mass Transfer* **23,** 451–460 (1979).
7. M. Hason and A. S. Mujumdar, Coupled heat and mass transfer in natural convection under flux condition along a vertical cone, *Int. Commun. Heat Mass Transfer* **11,** 157–172 (1984).
8. J. Srinivasan and D. Angirasa, Numerical study of double-diffusive free convection from a vertical surface, *Int. J. Heat Mass Transfer* **31,** 2033–2038 (1988).
9. T. S. Lee, P. G. Parikh, A. Acrivos and P. Bershader, Natural convection in a vertical channel with opposing buoyancy forces, *Int. J. Heat Mass Transfer* **25,** 499–511 (1982).
10. C. J. Chang, T. F. Lin and W. M. Yan, Natural convection flows in a vertical open tube resulting from combined buoyancy effects of thermal and mass diffusion, *Int. J. Heat Mass Transfer* **29,** 1453–1552 (1986).
11. W. M. Yan and T. F. Lin, Effect of wetted wall on natural convection heat transfer between vertical parallel plates, *Wärme- und Stoffübertr.* **23,** 259–266 (1988).
12. T. F. Lin, C. J. Chang and W. M. Yan, Analysis of combined buoyancy effects of thermal and mass diffusion on laminar forced convection heat transfer in a vertical tube, *J. Heat Transfer* **110,** 337–344 (1988).
13. W. M. Yan and T. F. Lin, Effects of wetted wall on laminar mixed convection in a vertical channel, *J. Thermophys. Heat Transfer* **3,** 94–96 (1989).
14. W. M. Yan, Y. L. Tsay and T. F. Lin, Simultaneous heat and mass transfer in laminar mixed convection flows between vertical parallel plates with asymmetric heating, *Int. J. Heat Fluid Flow* **10,** 262–269 (1989).
15. L. C. Chow and J. N. Chung, Evaporation of water into a laminar stream of air and superheated steam, *Int. J. Heat Mass Transfer* **26,** 373–380 (1983).
16. J. Schroppel and F. Thiele, On the calculation of momentum, heat, and mass transfer in laminar and turbulent boundary layer flows along a vaporizing liquid film, *Numer. Heat Transfer* **6,** 475–496 (1983).
17. C. H. Wu, D. C. Davis, J. N. Chung and L. C. Chow, Simulation of wedge-shaped product dehydration using mixtures of superheated steam and air in laminar flow, *Numer. Heat Transfer* **11,** 109–123 (1987).
18. W. M. Yan and T. F. Lin, Combined heat and mass transfer in laminar forced convection channel flows, *Int. Commun. Heat Mass Transfer* **15,** 333–344 (1988).
19. K. Suzuki, Y. Hagiwara and T. Sato, Heat transfer and flow characteristics of two-component annular flow, *Int. J. Heat Mass Transfer* **26,** 597–605 (1983).
20. W. W. Baumann and F. Thiele, Heat and mass transfer in two-component film evaporation in a vertical tube, *Proc. 8th Int. Heat Transfer Conf.*, San Francisco, Vol. 4, pp. 1843–1848 (1986).
21. T. R. Shembharkar and B. R. Pai, Prediction of film cooling with a liquid coolant, *Int. J. Heat Mass Transfer* **29,** 899–908 (1986).
22. M. Haji and L. C. Chow, Experimental measurement of water evaporation rates into air and superheated steam, *J. Heat Transfer* **110,** 237–242 (1988).
23. H. Perez-Blanco and W. A. Bird, Study of heat and mass transfer in a vertical-tube evaporative cooler, *J. Heat Transfer* **106,** 210–215 (1984).
24. J. R. Conder, D. J. Gunn and M. A. Shaikh, Heat and mass transfer in two-phase flow—a mathematical model for laminar film flow and its experimental validation, *Int. J. Heat Mass Transfer* **25,** 1113–1126 (1982).
25. W. M. Yan and T. F. Lin, Evaporative cooling of liquid film through interfacial heat and mass transfer in a vertical channel—II. Numerical study, *Int. J. Heat Mass Transfer* **34,** 1113–1124 (1991).

26. L. S. Marks, *Mechanical Engineers' Handbook*, p. 368. Hemisphere/McGraw-Hill, New York (1951).
27. W. M. Yan, Buoyancy induced heat and mass transfer in vertical channel flows, Ph.D. Thesis, Department of Mechanical Engineering, National Chiao Tung University, Hsinchu, Taiwan, R.O.C., January (1989).

REFROIDISSEMENT EVAPORATIF D'UN FILM LIQUIDE PAR TRANSFERT INTERFACIAL DE CHALEUR ET DE MASSE DANS UN CANAL VERTICAL—I. ETUDE EXPERIMENTALE

Résumé—Une étude expérimentale est conduite pour déterminer le refroidissement évaporatif d'un film liquide par transfert interfacial de chaleur et de masse dans un canal vertical. La température pariétale, les flux de chaleur et de masse sont présentés pour des systèmes avec évaporation d'un film d'eau et évaporation d'un film d'éthanol dans des larges domaines de débit-masse, de largeur de canal et de température d'entrée du liquide. Les résultats montrent que les influences de transfert par chaleur latente sur le refroidissement du film liquide dépendent beaucoup de la température d'entrée du liquide et du débit-masse. Le refroidissement efficace correspond à une température d'entrée élevée du film et à un faible débit-masse.

VERDUNSTUNGSKÜHLUNG AN DER OBERFLÄCHE EINES FLÜSSIGKEITSFILMS IN EINEM SENKRECHTEN KANAL—I. EXPERIMENTELLE UNTERSUCHUNG

Zusammenfassung—Es wird über eine experimentelle Untersuchung der Verdunstungskühlung durch gekoppelten Wärme- und Stofftransport an der Oberfläche eines flüssigen Rieselfilms in einem senkrechten Kanal berichtet. Für Systeme mit Verdampfung an einem Wasserfilm und einem Äthanolfilm werden Meßergebnisse für die Wandtemperatur sowie für den Wärme- und Stoffstrom vorgestellt. Dies geschieht für weite Bereiche des Flüssigkeitsmassenstroms, der Kanalbreite und der Flüssigkeits-Eintrittstemperatur. Die Ergebnisse zeigen, daß die Einflüsse der Verdunstung auf die Abkühlung des Flüssigkeitsfilms stark von der Film-Eintrittstemperatur und vom Flüssigkeitsmassenstrom abhängen. Günstige Bedingungen bestehen bei hoher Eintrittstemperatur und kleinem Massenstrom.

ИСПАРИТЕЛЬНОЕ ОХЛАЖДЕНИЕ ЖИДКОЙ ПЛЕНКИ В ВЕРТИКАЛЬНОМ КАНАЛЕ—I. ЭКСПЕРИМЕНТАЛЬНОЕ ИССЛЕДОВАНИЕ

Аннотация—Экспериментально исследуется испарительное охлаждение жидкой пленки, стекающей в вертикальном канале. Отдельно для случая испарения водяной пленки и для испарения пленки этанола приводятся экспериментально полученные значения температуры стенки и скорости тепло- и массопереноса для широких диапазонов изменения массового расхода жидкости, ширины канала и температуры жидкости на входа. Результаты показывают, что влияние скрытой теплоты парообразования на охлаждение жидкой пленки сильно зависит от температуры жидкой пленки на входе и массового расхода жидкости. Эффективность испарительного охлаждения повышается при увеличении начальной температуры жидкой пленки и уменьшении массового расхода жидкости.